POLITECNICO
MILANO 1863

SCUOLA DI INGEGNERIA INDUSTRIALE
E DELL'INFORMAZIONE

Executive Summary of the Thesis

Relationship between attenuation and phase delay due to rain in the 10-100 GHz frequency range

Laurea Magistrale in Space Engineering - Ingegneria Spaziale

Author: Salim Abboudi

Advisor: Prof. Lorenzo Luini

Academic year: 2021-2022

1. Introduction

Shifting to new high frequency bands typically above 10 GHz like Ka, Q or even V bands has became recently vital to comply with the increasing demands in high bandwidth, data rate and availability but more importantly to overcome the lower frequency bands 's crowding, the next future wireless telecommunications systems are expected to provide reel time multimedia availability to meet with ever increasing customer services However the higher frequencies are considerably affected by rainfall; attenuation and phase delay are major aspects putting in jeopardy the user requirements meeting, therefore it is necessary to mitigate rain attenuation to ensure the quality of the link, to this purpose, dynamic attenuation mitigation methods or fade mitigation techniques(FMT)[2] are implemented alongside attenuation prediction models to predict the projected attenuation of the link. Many studies have been conducted on this issue worldwide,where by investigating geographically distributed locations, we can develop and analyze rain attenuation models applicable over a wide frequency range, apply FMT first, plan the link budget and finally design the system ensuring the best quality for the service.

It was shown that rain attenuation could reduce the throughput of a link compared to sunny weather conditions, likely by deploying an appropriate rain attenuation model, even in the rain, a terrestrial link's throughput can be kept unchanged compared to a case without deploying any FMT and with the condition that other parts are usually working, an appropriate model requires the collection of factors impacting attenuation like path length, frequency, elevation angle, polarisation angle, rain drop size distribution (DSD)... Thus, rain attenuation models play a significant role in the FMT operation in a transmission system.

Several measurements and modeling of rain attenuation exist in the literature, this abundance unlikely is faced by a rarity of phase delay models, the reason why deriving a relationship linking the latter to attenuation is crucial. This work aims then at presenting an analytical model linking attenuation to delay due to rain as a function of different drop size distributions in the 10-100 GHz range.In fact, we explore the EXCELL model [3] to generate some data for both attenuation A and phase delay τ, we explore then the main parameters influencing the scatter plot $\tau = f(A)$, and then we fit the data using suitable laws. Finally, we compute the fitting error and refine the model.

2. Attenuation and phase delay model

This section addresses the method followed to build the analytical model $\tau = f(A)$, we will present the rain rate model EXCELL, then discuss how the τ, A data is generated. This data is analyzed varying certains parameters and finally the analytical model is derived fitting the data to the main parameters using suitable laws.

2.1. EXCELL Model

This model describes the horizontal rain structure that can be determined based on the local statistical distribution of the point rainfall intensity, the exponential cell is characterized by 2 parameters R_M and ρ_0 representing the maximum rain rate inside the cell and its equivalent radius i.e the radius for which the rain rate decreases by a factor of e^{-1}. The rain rate profile inside one cell in fig. 1 can be expressed as :

$$R(\rho) = R_M \exp\left[-\rho/\rho_0\right]. \tag{1}$$

The radius of the cell is constrained by a threshold value R_{th} fixed to $0.5mm/h$. Hence, the radius of the cell can be written :

$$r_{cell} = \rho_0 \, log(\frac{R_M}{R_{th}}) \tag{2}$$

In cartesien coordinate, the rain rate is a matrix 2d whose resolution dr depends on the rain cell radius :

$$dr = \frac{r_{cell}}{30} \tag{3}$$

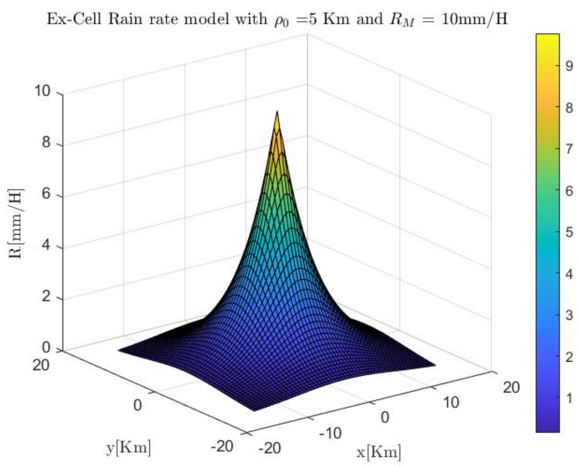

Figure 1: Excell rain rate Profile

2.2. Specific attenuation and phase delay

Since the propagation factor in a rain medium is $\exp(-\gamma r)$,where γ is the propagation constant, the real $\Re$ and imaginary part $\Im$ of γ are respectively responsible for attenuation and phase shift of the wave propagating in the rain medium. The specific attenuation due to rain γ_R, and specific phase delay due to rain φ_R, are then given in dB/km and deg/km.

[6] provides an empirical procedure based on the approximate relation between γ (dB/km) and rain rate R (mm/h), which is fitted by Laws and Parsons (L-P) distribution, the relationship between specific attenuation γ and rain rate R is described with a power law:

$$\gamma_R = kR^{\alpha} \tag{4}$$

Similarly, an empirical procedure based on the approximate relation between φ_R (deg/km) and rain rate R (mm/h) can be used, which is fitted by Laws and Parsons (L-P) distribution, the relationship between the phase dur to rain and rain rate R with a power-law is:

$$\varphi_R = hR^{\beta} \tag{5}$$

Where R is the rain rate in eq. (1) and k, α, h, β are coefficients that depend on: frequency f, elevation angle θ, polarization angle: ψ and drop size distribution(DSD). This analytical dependency has been carried in the thesis [5] and constitutes an important milestone in our work.

Finally, the phase can be linked to the phase delay in picoseconds and frequency f in GHz

$$\tau_R = \frac{1000}{360f} \varphi_R \tag{6}$$

2.3. Attenuation and phase delay data

let H_R be the rain height, and θ the link elevation angle,from fig. 2, we can write :

$$L_H = cos(\theta)L \qquad H_R = tan(\theta)L_H \tag{7}$$

The attenuation along the slant path is :

$$A = \int_L \gamma_R \propto \int_{L_H} kR^{\alpha} \tag{8}$$

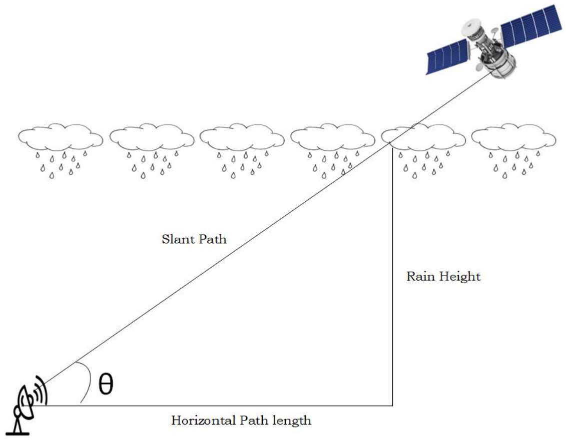

Figure 2: Sketch slant path and elevation angle

Whilst the delay can be written as

$$\tau = \frac{1000}{360f}\int_L \varphi_R \propto \frac{1000}{360f}\int_{L_H} hR^\beta \qquad (9)$$

In fact, in fig. 3 we can see the rotational profile of the EXCELL model, whose peak is in the center,and cell radius covers the map dimension. Simulating two random positions of the satellite and the station inside the EXCELL cell, we can equivalently(thanks to eq. (7) perform integration along their relative distance (horizontal path length L_H) eqs. (8) and (9)
Thus, for a fixed L_H, the one cell approach leads to a couple (τ, A). In order to simulate all the scenarios, i.e all the possible L_H between the ground station and the satellite , we move the satellite mapping all the possible points in the map, for each scenario we get a couple (τ, A), hence for each EXCELL map (R_M, ρ_0), we get a vector of attenuations and phase delays that we can plot in a scatter plot fig. 4

The plot in fig. 4 shows that the trend is a power law for a cell with parameters $(R_M, \rho_0) = (20mm/h, 2km)$. Since our model should not depend on a single rainfall scenario, we would like to see the trend for different R_M, ρ_0, we plot also the curve fitting all the data using the matlab command fit(A,τ,'Power') fig. 5 shows that the power law fits well the scatter plot τ-A and does not depend on(R_M, ρ_0), thus the red curve is the one representing *data*, this curve represents the $\tau - A$ relationship for certain values of : frequency -elevation angle-rain height- polarisation angle- drop size distribution (DSD), for

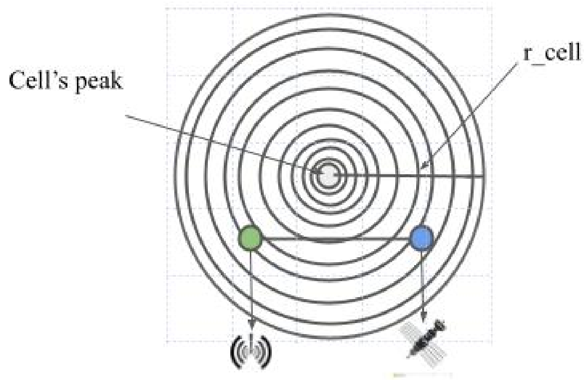

Figure 3: Satellite and station inside EXCELL

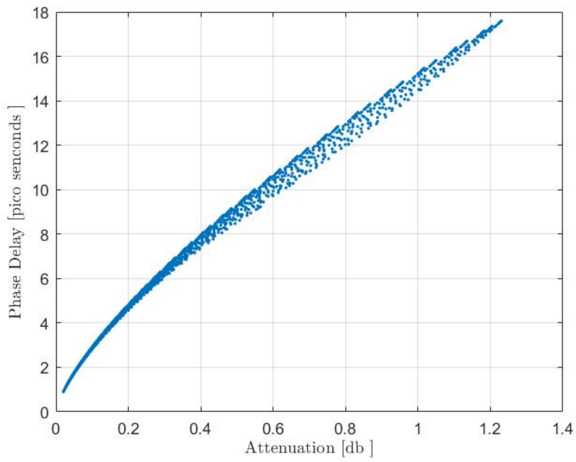

Figure 4: τ-A plot for

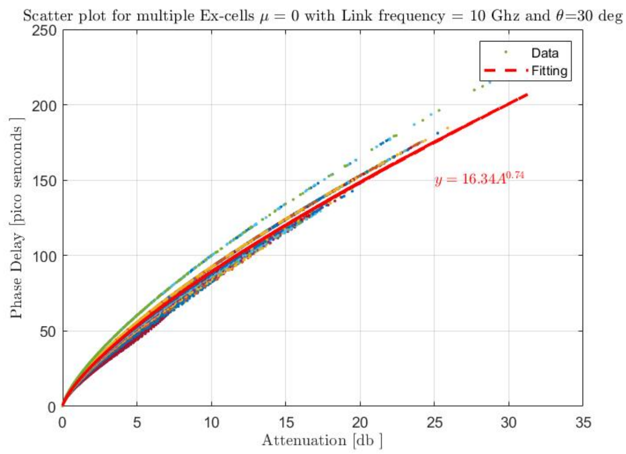

Figure 5: Multi-cell approach Fitting

which we can get the coefficient a,b representing the power law $\tau = aA^b$

2.4. Data fitting

The parameters used to generate the data were the one used in [5] i.e: frequency f,elevation Angle θ,the parameter μ characterizing the gamma DSD, polarisation angle ψ and rain Height H_R influencing attenuation and delay through L_H eq. (7). We have analyzed how the curve *Data* is influenced varying the parameters and we noticed that μ and θ have a noticeable impact on the data, whilst θ, H_R barely have an influence so they were combine a new variable L_H: eq. (7) and ψ doesn't have any influence,it was fixed therefore. We have then to find a and b :

$$\begin{cases} \psi = 45° \\ L_H = \frac{H_R}{\tan(\theta).} \\ \tau = a((f, L_H, \mu) \;\; A^{b(f, L_H, \mu)} \end{cases} \tag{10}$$

Since the value $\mu = 0$ is the most probable one for the gamma distribution, we focus only on it in this work.

$$\mu = 0 \tag{11}$$

For each frequency,and horizontal path, we generate the data,we fit it with a classical power law, and we plot the variation of both a and b, this variation helps us to predict the fitting model for a and b to frequency first, and then the coefficients of the first fitting to horizontal path. The model proposed, as a function of frequency is a power law for a and a polynomial for b.

$$\begin{cases} a(f) = a_1 f^{a_2} \\ b(f) = b_1 f^4 + b_2 f^3 + b_3 f^2 + b_4 f + b_5 \end{cases} \tag{12}$$

And a polynomial of the fifth degree depending on L_H for $a_1, a_2, b_1, b_2, b_3, b_4, b_5$

$$\forall i \in \{1, 2\} \quad a_i = \sum_{j=0}^{5} a_{ij} L_H^j \tag{13}$$

$$\forall i \in \{1, 2, 3, 4, 5\} \quad b_i = \sum_{j=0}^{5} b_{ij} L_H^j \tag{14}$$

3. Error Computation

In this section, we compute the error of the model, using two approaches, the first one hinges on the accuracy of the *data* curve vs the analytical model, and the second recalls the SC-EXCELL to calculate the error through the attenuation measured cumulative distribution function(ccdf) and the phase delay ccdf for the site of Milan.

3.1. EXCELL based error

The error figure used has been defined by ITU-R P.311-13 [1] to deal with low value of attenuation, but can be used also for phase delay τ_{data} is the data phase delay,and $\tau_{analy}$is the phase delay found from eq. (10), the error eq. (15) is calculated for each frequency,in the range 10-100 GHz, and horizontal path in the range [0,13.43 km] found from eq. (7); θ varies in the range [20°.90°]

$$\varepsilon = \begin{cases} 100\left(\frac{\tau_{data}}{10}\right)^{0.2} \ln\left(\frac{\tau_{analy}}{\tau_{data}}\right) & \tau_{data} < 10ps \\ 100 \ln\left(\frac{\tau_{analy}}{\tau_{data}}\right) & \tau_{data} \geq 10ps \end{cases} \tag{15}$$

In fig. 6,we plot the rms of the error ϵ The error

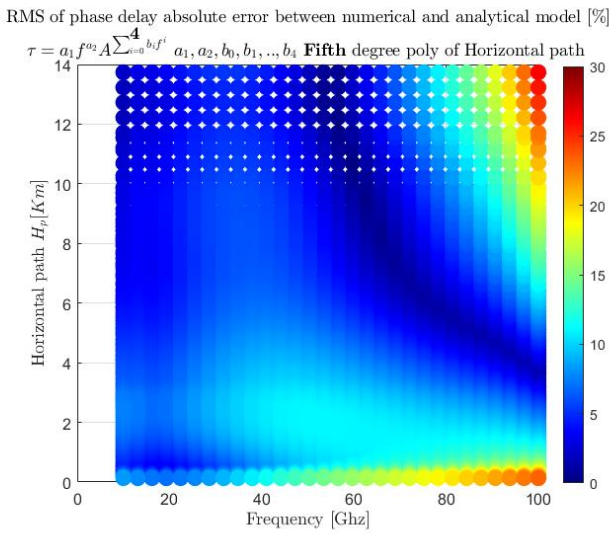

Figure 6: Root mean square of the error figure

shows globally that the model is globally producing accurately the data, with a mean value of 8% . The plots shows 2 critical regions where the rms of the error is higher than 20 % :

- very short horizontal path L$_H$ $\leq$ 0.7 Km i.e high elevation angles θ for a fixed rain height and high frequencies (70-100) GHz
- High horizontal path L$_H$ $\geq$ 10 Km i.e low elevation angles θ for a fixed rain height and very high frequencies (90-100) GHz

3.2. SC-EXCELL based error

One of the applications of the SC-EXCELL model [4] is its probabilistic approach through the cumulative distribution functions of attenuation and phase delay, we take advantage from this to evaluate the accuracy of our analytical model $\tau = g(A)$through measured data (ccdfs) in the site of Milan. The idea is to generate the attenuation cumulative distribution function $F_A(t)$ and the phase delay ccdf $F_\tau(t)$ and compare look at the same probability level P and compare τ giving F_τ which is noted as τ_{data} and $\tau_{analy} = g(A)$where A giving F_A, the error can be defined in the same way as before for a certain probability level P eq. (15)

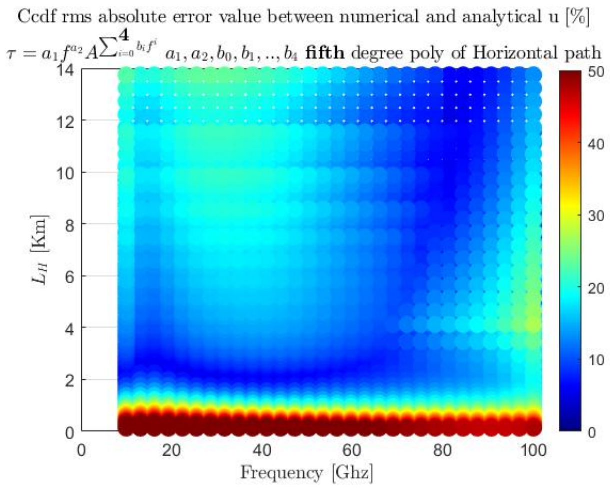

Figure 7: CCDF rms of the error between Analytical and experimental phase delay

In fig. 7, the mean value of the rms is around 13.84 % , the maximum value is 63.55% while the minimum value is 0.88 %, we also notice, likewise the first approach, the plot shows that for $L_H < 1$ the error is around 45 % which constitute a layer to exclude definitely. The error outside the red region has a mean value of only 6% showing thus a great fitting for the analytical model.
In fig. 8, we picked an example in the red region, we can clearly see how inaccurate is the model.

4. Model refinement

As we saw before, there are certain regions where the model is inaccurate, thus we try to limit frequency and horizontal path so that the model gets globally better.2 regions are concerned

1. The region $L_H \leq 1$ in fig. 7 has to be discarded since the average rms in there is around 45%

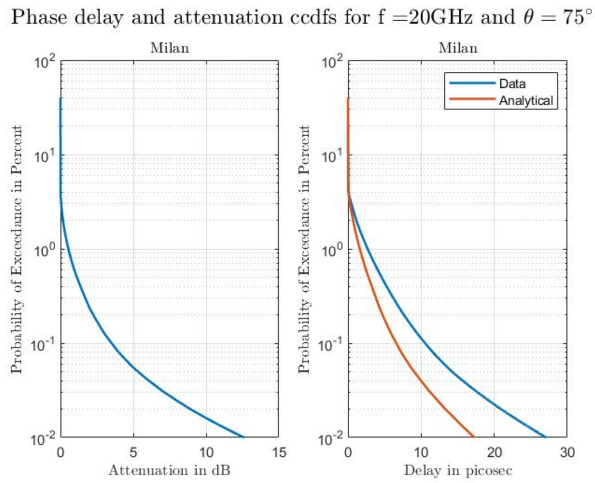

Figure 8: ccdf plot comparison vs data

2. The region $f \geq 90$ GHz in fig. 6 has to be discarded since the average rms in there is around 20%

In tables 1 and 2 we present the final results of the error analysis within the new domain of validity. As we can see, both approaches show similar mean value for the error, we can confirm that the model is accurate for both approaches.

Table 1: Error between model and data

	Error RMS		
	Mean	Min	Max
EXCELL based Comparison	**7.36%**	0.06 %	15.9 %

Table 2: Error between model and data

	Error RMS		
	Mean	Min	Max
SC-EXCELL based Comparison	**8.19%**	0.88%	23.55%

Remark The model obtained was derived by an iterative process, where we started from a more complex models in eq. (12),eq. (13) and eq. (14), and each time we calculate the mean of the error figure root mean square for both approaches, we stop until we achieve a mean rms of 10 % for both,

$$mean(rms(\epsilon)) \leq 10\% \tag{16}$$

The model presented in this paper was then the best compromise between accuracy(eq. (16)) and complexity(the numbers of coefficients involved), we had moreover to shrink its domain of validity to fully meet the requirement eq. (16)

Finally, the full model, whose coefficients can be found in appendix A, can be written as:

$$\begin{cases} \underline{\textbf{Data}} : \psi = 45°, \mu = 0 \\ \underline{\textbf{Model}} \\ \qquad \tau = a_1 f^{a_2} A^{b_1 f^4 + b_2 f^3 + b_3 f^2 + b_4 f + b_5} \\ \qquad a_1(L_H) = \sum_{j=1}^{j=6} a_{1j} L_H^{j-1} \\ \qquad a_2(L_H) = \sum_{j=1}^{j=6} a_{2j} L_H^{j-1} \\ \qquad \forall i \in \{1, 2, ..5\} \quad b_i(L_H) = \sum_{j=1}^{j=6} b_{ij} L_H^{j-1} \\ \underline{\textbf{Constrains}} : 10\, GHz \leq f \leq 90\, GHz \\ \qquad\qquad L_H \geq 1Km \end{cases}$$

5. Conclusions

This thesis work could be one of the applications of the cellular model EXCELL developed in 1981 by capsoni, in fact, we saw that starting from a simple exponential law for rain rate distribution, and simple power laws for specific attenuation and phase delay that we can integrate on the slant path to get both attenuation and delay, we can build a general analytical model linking attenuation to phase delay depending on frequency, horizontal path and DSD.
The study deals with $\mu = 0$ since it's the most probable one for the gamma distribution DSD. In the error computation, we have used 2 different approaches to confront the model, the first is based on the data found using the EXCELL model , while the second recalled the SC-EXCELL output in terms of exceedance probability for both attenuation and delay to rate the accuracy of the analytical model.The last stage was to refine the model to meet the requirement of accuracy. The study concluded that the model chosen has a rms error of 7.36 % and 8.19 % for the theoretical and the experimental approach respectively .

References

[1] Presentation Acquisition. Analysis of data in studies of tropospheric propagation. *Recommendation ITU-R*, pages 311–10, 2009.

[2] Ana Vazquez Alejos, Manuel Garcia Sanchez, and Inigo Cuinas. Propagation impairments mitigation techniques for broadband wlans. In *The Second European Conference on Antennas and Propagation, EuCAP 2007*, pages 1–4. IET, 2007.

[3] C Capsoni, F Fedi, C Magistroni, A Paraboni, and A Pawlina. Data and theory for a new model of the horizontal structure of raincells for propagation applications. *NASA STI/Recon Technical Report N*, 89:17785, 1988.

[4] Carlo Capsoni, Lorenzo Luini, Aldo Paraboni, Carlo Riva, and Antonio Martellucci. A new prediction model of rain attenuation that separately accounts for stratiform and convective rain. *IEEE Transactions on Antennas and Propagation*, 57(1):196–204, 2009.

[5] GUANJUN LI. An analytical model for the attenuation and phase delay due to rain in the 6-100 ghz range. 2022.

[6] D Maggiori. Computed transmission through rain in the 1-400 ghz frequency range for spherical and elliptical drops and any polarization. *Alta Frequenza*, 50:262–273, 1981.

A. Appendix

Table 3: Analytical Model for $\mu = 0$

$\mu = 0$	$\tau = aA^b$						
Model	$a = a_1 f^{a_2}$		$b = b_1 f^4 + b_2 f^3 + b_3 f^2 + b_4 f + b_5$				
	a_1	a_2	b_1	b_2	b_3	b_4	b_5
	$\sum_{j=1}^{j=6} c_j L_H^{j-1}$	$\sum_{j=1}^{j=6} c_j L_H^{j-1}$	$\sum_{j=1}^{j=6} c_j L_H^{j-1}$	$\sum_{j=1}^{j=6} c_j L_H^{j-1}$	$\sum_{j=1}^{j=6} c_j L_H^{j-1}$	$\sum_{j=1}^{j=6} c_j L_H^{j-1}$	$\sum_{j=1}^{j=6} c_j L_H^{j-1}$
c_6	0.0142	-1.61 10^{-6}	-2.05 10^{-14}	3.6 10^{-12}	-7.6 10^{-11}	-1.9 10^{-8}	1.56 10^{-6}
c_5	-0.589	6.5 10^{-5}	6.09 10^{-13}	-9.82 10^{-11}	-2.68 10^{-11}	7.4 10^{-7}	-5.78 10^{-5}
c_4	9.456	-1.04 10^{-3}	-4.87 10^{-12}	5.36 10^{-10}	6.75 10^{-8}	-1.1 10^{-5}	8 10^{-4}
c_3	-73.44	0.008	-4.45 10^{-12}	4.95 10^{-9}	-1.1 10^{-6}	8.1 10^{-5}	-0.0055
c_2	292.5	-0.026	1.46 10^{-10}	-4.6 10^{-8}	5.51 10^{-6}	-2.7 10^{-4}	0.0155
c_1	305.7	-1.686	-9 10^{-9}	2.13 10^{-6}	-2 10^{-4}	0.005	0.696